



Polymer Reinforced DNAN/RDX Energetic Composites: Interfacial Interactions and Mechanical Properties

Wen Qian, Xizhou Chen,* Guan Luo**

Institute of Chemical Materials, China Academy of Engineering Physics (CAEP), Mianyang 621900, China

*E-mails: *chen_xizhou@hotmail.com; **luoguan@caep.cn*

Abstract: 2,4-Dinitroanisole (DNAN) has excellent properties as a replacement for 1,3,5-trinitrotoluene (TNT) in melt-cast explosives, and the polymeric modifier used is critical to the mechanical modification of the DNAN/RDX energetic composite. In our research, the typical polymeric modifier acrolein-pentaerythritol resin (APER) was successfully added experimentally to the DNAN/RDX system, and the effects of interfacial interactions on the mechanical properties of these polymers in reinforcing the DNAN/RDX energetic composites were investigated by molecular dynamics simulations, scanning electron microscopy (SEM) and mechanical testing. The results showed that strong attractive interactions exist between the polymer and the explosives, wherein van der Waals forces were found to play the main role. The morphological micro-images also showed tight binding between the polymer/explosive interfaces, which supported the calculated strong interfacial interactions. The mechanical tests confirmed that adding the polymers can obviously reinforce the mechanical strength and toughness of DNAN/RDX systems. The above observations revealed that the cooperative effects of the APER polymer can help to reinforce the interfacial interactions and mechanical properties of DNAN/RDX composites, which is of importance in the formulation and mechanical evaluation of advanced energetic composites.

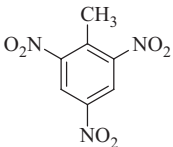
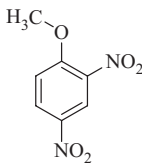
Keywords: energetic composites, dinitroanisole, molecular dynamics, interfacial interaction, mechanical property

1 Introduction

As one of the most suitable candidates for the continuous phase replacement of 1,3,5-trinitrotoluene (TNT) in melt-cast composite explosives, 2,4-dinitroanisole

(DNAN) has attracted researchers' attention because of its excellent properties, such as low-melting-point, low-sensitivity, and low-shrinkage [1-3]. As shown in Table 1, compared with the molecular structure of TNT, a DNAN molecule has an anisole (methoxybenzene) core with two nitro groups attached, and exhibits a low-melting-point and high-energy, similar to TNT. Moreover, DNAN can reduce the sensitivity, with little energy or density loss, for energetic composites compared with the traditional TNT-based composites [2, 3]. In addition, the traditional fabrication equipment and methods used for TNT can be used in the fabrication of DNAN [4-6]. A series of DNAN-based energetic composites has been developed, such as the PAX series, and PAX charged weapons have been utilized in military ordnance; other formulations include ARX-4027, which contains 39.75% DNAN and 60% 1,3,5-trinitroperhydro-1,3,5-triazine (RDX) [7-11].

Table 1. Comparison of DNAN with TNT

Properties	TNT	DNAN
Structure		
Density [g/cm ³]	1.654	1.336
Melting point [K]	355	367
Heat of formation [kJ/mol]	-58.576	-184.096
Detonation velocity [m/s]	6825	5974
Shock sensitivity ^a [cm]	157.0	117.5
Oxygen balance ^b [%]	-74.0	-96.9

^a Drop height for 50% explosion probability (H₅₀), 5 kg; ^b OB_{CO₂}.

However, because of the low density and low viscosity of DNAN [12-14], solid-liquid phase dislocations may appear during processing of a composite when using DNAN as the continuous phase, which will induce degradation of the solid phase, and affect the mechanical properties of the energetic composite, leading to weak dimensional stability, poor toughness and high brittleness [15-17]. Molecular simulations and mechanical tests of TNT and DNAN show that the compressive strength, tensile strength, shear strength and plastic deformation of DNAN are all lower than those of TNT, thus DNAN is more prone to brittle fracturing compared with TNT [18]. Mechanical modifiers, especially polymeric modifiers are key to solving this problem [19]. Thermosetting polymers, such

as acrolein-pentaerythritol resin (APER), have excellent mechanical sensitivity, good dimensional stability and heat resistance, and explosive products containing them are difficult to soften and deform, thus they will have good storability and overall performance [20-22]. Combining the advantages of the casting process and the plastic bonded effect, we can obtain a type of insensitive energetic composite.

As for the design and mechanical modification of composite materials, it is efficient to combine the advantages of theoretical calculations and experimental results, and it is helpful to consider the effects of interfacial interactions and morphologies on the mechanical performance of the whole system. Thus in our study, typical polymer modified, APER reinforced DNAN-based composites were investigated both theoretically and experimentally, the interfacial interactions and mechanical properties were discussed, and the results will be of great importance for formulation of advanced melt-cast explosives.

2 Simulation and Experimental Details

2.1 Structure modelling

The crystal structures were constructed based on the experimental data from Cambridge Crystallographic Data Center (CCDC). DNAN [23] belongs to the monoclinic system and $P_{21/N}$ space group, with lattice parameters $a=0.8772$ nm, $b=1.2645$ nm, $c=1.5429$ nm, and $\beta=81.89$ (Figure 1a), and α -RDX [24] belongs to the orthorhombic system and P_{BCA} space group, with lattice parameters $a=1.3182$ nm, $b=1.1574$ nm, and $c=1.0709$ nm (Figure 1b). The DNAN molecular structure (Figure 1c) was abstracted from the DNAN crystal.

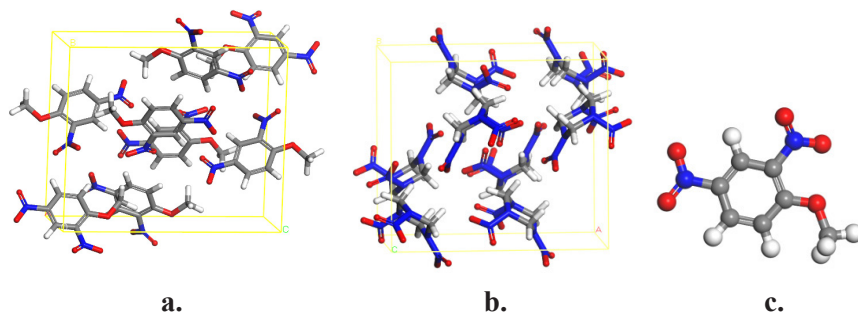


Figure 1. Molecular structures of the DNAN crystal (a), RDX crystal (b), DNAN molecule (c) [Atom colours: Carbon (grey), Hydrogen (white), Oxygen (red), Nitrogen (blue)]

As for polymer modelling, simplified models were constructed as follows: the molecular configuration of APER containing two prepolymer structures (Figures 2a and 2b) was constructed in the way of a dendrimer [25], then the structures were geometrically-optimized and energy-minimized under the Condensed-phase Optimized Molecular Potentials for Atomistic Simulation Studies (COMPASS) forcefield. This force field is applicable to various organic molecules and groups [26, 27] (Supporting Information, SI). The optimized structure with minimized energy is shown in Figure 2c.

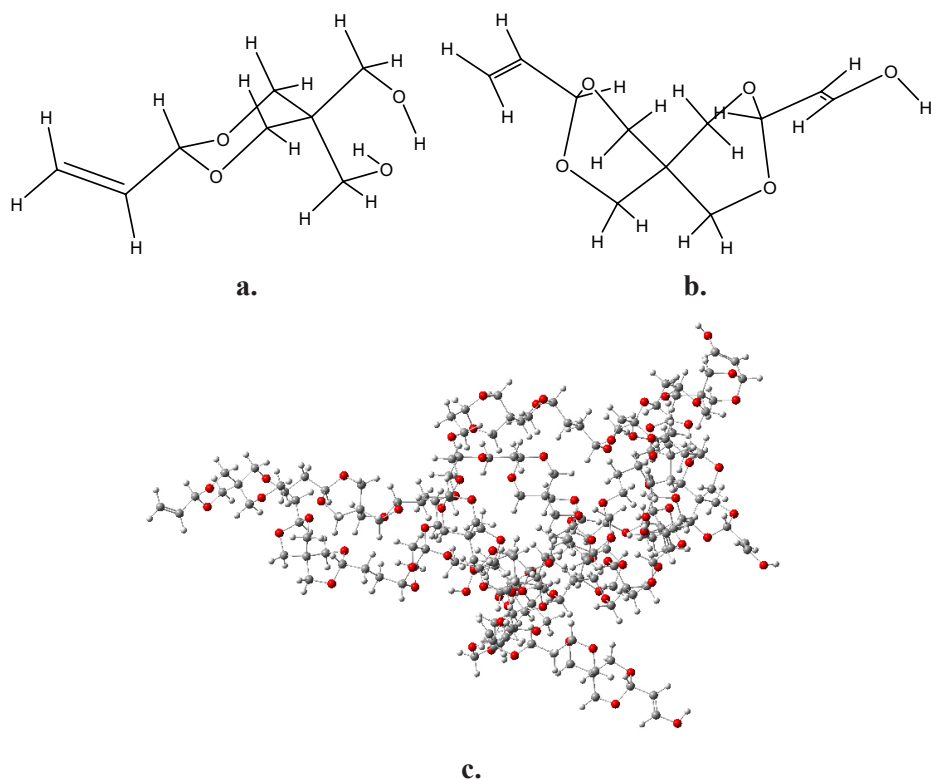


Figure 2. Chemical formulae for two prepolymer structures (a), (b), and the molecular model (c) of APER

2.2 Prediction of crystal habits

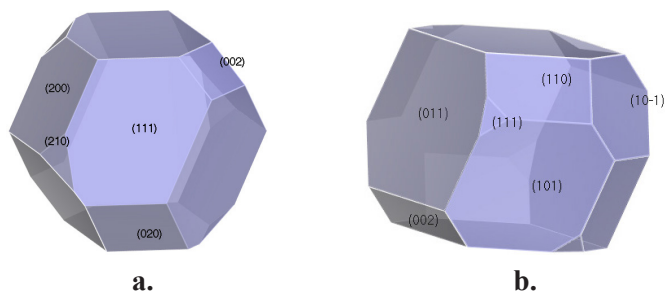


Figure 3. Predicted crystal habits for α -RDX (a) and DNAN (b)

In the formed energetic composites, the polymers were mixed with solid DNAN and RDX crystals. Firstly, Bravais-Friedel Donnay-Harker (BFDH) [28-30] calculations were carried out on the primitive cells of RDX and DNAN at ultra-fine level, and possible growth faces and their relative growth rates, depending only on the crystal lattice and symmetry, were predicted, as shown in Figure 3 and Table 2. In order to investigate the interfacial interactions along different crystal directions, a $4 \times 3 \times 2$ DNAN supercell and a $3 \times 3 \times 3$ RDX supercell were constructed, based on the primitive cells. Then the supercell was cleaved along the main crystal faces (0 1 1), (1 0 1), (1 1 0), (1 0 -1) and (0 0 2) for DNAN, and (0 2 0), (2 0 0), (2 1 0), (1 1 1) and (0 0 2) for RDX, according to the BFDH method for predicted crystal habits.

Table 2. Predicted crystal habit for α -RDX and DNAN

RDX (h k l)	Multiplicity	D_{hkl} [nm]	Distance [nm]	Total facet area [nm ²]	Facet area [%]
(1 1 1)	8	0.675	1.481	28.4979	74.08
(2 0 0)	2	0.659	1.517	4.9574	12.89
(0 2 0)	2	0.579	1.728	2.7744	7.21
(2 1 0)	4	0.573	1.746	1.0030	2.61
(0 0 2)	2	0.535	1.868	1.2359	3.21
DNAN (h k l)	Multiplicity				
(0 1 1)	4	0.974	1.027	13.0245	53.70
(1 0 1)	2	0.805	1.242	4.0850	16.84
(1 1 0)	4	0.716	1.397	3.1570	13.02
(1 0 -1)	2	0.713	1.403	2.1928	9.04
(0 0 2)	2	0.764	1.309	1.5671	6.46

2.3 Calculation of interfacial interactions

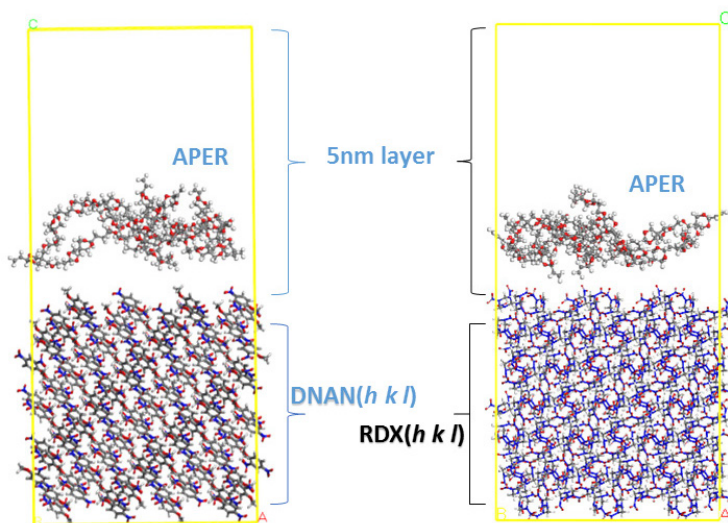


Figure 4. Polymer/explosive-crystal solid interfacial models [DNAN(1 0 1), and RDX(1 1 1) taken as examples]

The optimized polymer segments with the density discussed above, along with a 5 nm vacuum layer, was introduced onto each crystal direction to construct the solid interfacial models, as shown in Figure 4. The structures were optimized by molecular mechanics (MM) and energy-minimized. Then molecular dynamics (MD) simulations were carried out on the optimized structures under NPT (with constant particle number, pressure and temperature) (100 ps), NVT (with constant particle number, volume and temperature) (500 ps) and NVE (with constant particle number, volume and energy) (500 ps) ensembles, with the COMPASS force field. Velocity Verlet arithmetic [31] was utilized; and the initial velocity was sampled by Maxwell distribution; the van der Waals force was calculated by the atom-based method and the Coulomb interaction was calculated by the Ewald method [32, 33]. To simulate normal conditions, the target temperature and pressure were set to 298 K and 100 kPa, and the Anderson method [34] was used to control the temperature and the Berendsen method [35] was used to control the pressure. The time increment was 1 fs. To ensure that the system is equilibrated properly, equilibrium both in energy and temperature is needed.

The interaction energies can be calculated from the final total energies of the explosive supercell, the polymer segment and the polymer/explosive-crystal model by the simplified equation [36]:

$$E_{\text{inter}} = E_{\text{total}} - (E_{\text{explosive}} + E_{\text{polymer}}) \quad (1)$$

where E_{inter} is the interaction energy, $E_{\text{explosive}}$, E_{polymer} and E_{total} are the total energies of the pure explosive-crystal, the polymer and the polymer/explosive-crystal respectively (kJ/mol). The contributions of van der Waals forces and electrostatic interactions (including hydrogen bonds) were given separately; here hydrogen bonds were a natural consequence of the standard van der Waals and electrostatic parameters and special hydrogen bond functions were not included (see SI). The interaction energies were normalized by the cross-sectional area, as shown in Equation 2:

$$E'_{\text{inter}} = E_{\text{inter}} / S \quad (2)$$

wherein E'_{inter} is the normalized interaction energy (kJ/mol), and S is the cross-sectional area of the optimized interface model (nm²). The absolute values of the interaction energies can determine the strength of the interfacial interactions [37, 38].

2.4 Experimental section

In order to investigate the mechanical properties of a DNAN-based system, experiments in fabrication and characterization for various DNAN-based composites were carried out. DNAN (purity 99%) was provided by Xiangfan Xindongfang Chemical Industry Co., Ltd. RDX (purity 99%, fine crystals with particle size 20-45 μm , coarse crystals with particle size 245-350 μm) was supplied by Gansu Yinguang Chemical Industry Co., Ltd. Acrolein-Pentaerythritol resin (APER) and its solidifier Diethyl sulfate (DES) were provided by Liming Research Institute of Chemical Industry.

The energetic composites consisted of molten DNAN (melted at 363-373 K with steam in a casting vessel) and RDX energetic crystals (DNAN:RDX=35:65 wt.%). Considering the effect of adding the polymer on the detonation performance, 0%, 1% (of wt. of DNAN/RDX) of polymer additives APER/DES were added; samples with 2%, 4% and 6% additives (which will not be used in industrial compositions) were also fabricated only to be compared with the 0% and 1% samples. Keeping the temperature at 373 K, the mixtures were stirred until the RDX and polymer additives were dispersed homogeneously in the molten DNAN slurry. The blends were then poured into preheated moulds and allowed to solidify for 2 h at ambient temperature; the polymer cross-linking reactions occurred during the curing process, forming test samples as shown in Figure 5. According to X-ray examination, the casting quality of the samples was good, without any obvious defects.

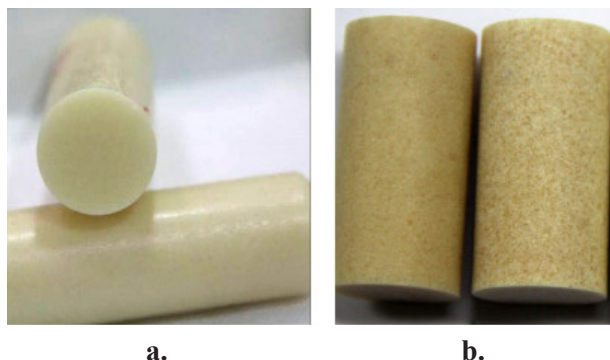


Figure 5. The DNAN-based energetic composite specimens (a) DNAN/RDX, (b) polymer modified DNAN/RDX

Mechanical tests were then carried out on the DNAN composite specimens using a Universal Testing Machine (Instron® 5582, UK) following the GJB-772A-97 standard method [39]; testing temperature was 293 K, and the cross-head speed was $0.1 \text{ mm} \cdot \text{min}^{-1}$, the samples should be processed into discs of 10 mm diameter and 20 mm thickness, thus the compressive/tensile strength and the percentage elongation of the energetic composites can be measured as follows. The compressive/tensile strength σ (MPa) is:

$$\sigma = F / S \quad (3)$$

where F is the total loading force at the point of cracking (kN), S is the cross-sectional area of the sample (cm^2). The percentage elongation δ (%) is:

$$\delta = (l - l_0) / l_0 \times 100\% \quad (4)$$

where l_0 is the original length of the sample (cm), l is the length of the sample after compression (cm).

The morphologies of the fractured surfaces of the samples were examined by scanning electron microscopy (SEM, Apollp 300, CamScan, UK) at an accelerating voltage of 12 kV, and the prepared surfaces were coated with Au in order to prevent charge build up on the specimen surfaces [40].

3 Results and Discussion

3.1 Interfacial interactions

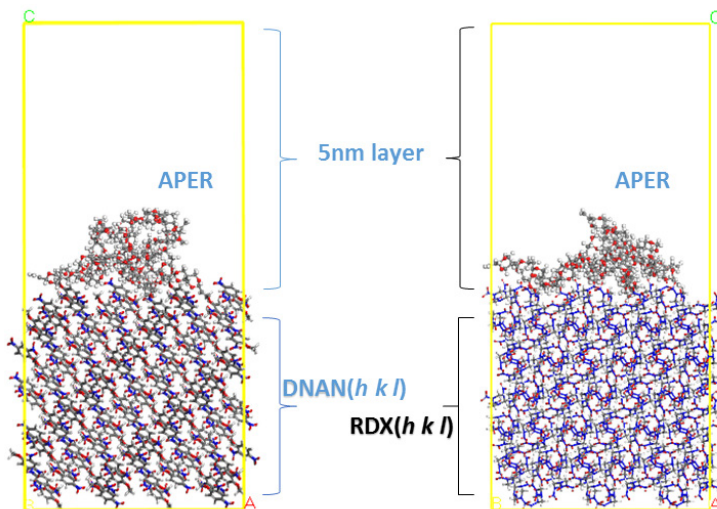


Figure 6. Optimized Polymer/DNAN solid interfacial models after molecular dynamics simulations [DNAN (1 0 1), and RDX (1 1 1) taken as examples]

Table 3. Interaction energy between polymeric modifier and RDX or DNAN

Direction	E_{inter} [kJ/mol]	S [nm ²]	E'_{inter} [kJ/mol·nm ²]	E'_{vdW} [kJ/mol·nm ²]	E'_{electro} [kJ/mol·nm ²]
DNAN(0 1 1)	-624.887	17.158	-36.419	-34.010	-1.709
DNAN(1 0 1)	-508.171	16.439	-30.913	-28.535	-1.344
DNAN(1 1 0)	-509.110	15.946	-31.928	-30.486	-1.439
DNAN(1 0 -1)	-477.682	18.925	-25.240	-23.169	-1.839
DNAN(0 0 2)	-502.118	13.311	-37.723	-35.661	-2.090
RDX(1 1 1)	-345.088	24.103	-14.317	-12.525	-1.619
RDX(2 0 0)	-503.599	11.155	-45.145	-43.511	-1.496
RDX(0 2 0)	-493.792	12.705	-38.866	-35.844	-1.552
RDX(2 1 0)	-481.710	25.674	-18.762	-17.237	-1.176
RDX(0 0 2)	-468.442	13.731	-34.115	-32.043	-1.923

According to the optimization and MD simulations of the interfacial structures, the distance between the polymer and DNAN system was reduced,

and the polymers were absorbed on the crystal face, as shown in Figure 6, showing that strong interfacial interactions exist between the polymer and the DNAN system. The interaction energy, normalized by cross-sectional area, can be calculated from the total energy of the equilibrium structures. The results are listed in Table 3.

It can be seen that strong interfacial interactions exist between the DNAN system and the polymer, where the van der Waals (vdW) forces contribute most to the total interactions, and electrostatic interactions contribute little; along different crystal faces, as shown in Figure 7, the attraction energies show anisotropy: for DNAN $(0\ 1\ 1) > (1\ 1\ 1) > (1\ 1\ 0) > (1\ 0\ 1) > (0\ 0\ 2)$, while for RDX $(2\ 0\ 0) > (0\ 2\ 0) > (2\ 1\ 0) > (0\ 0\ 2) > (1\ 1\ 1)$, which is caused by the different inter-molecular interaction situations along the different DNAN crystal faces. The layer-like structure of the DNAN crystal is the main reason for the anisotropic situations, which matches the situations in the equilibrium structures. In summary, the polymers have strong attractive interactions with the DNAN interfaces along different crystal directions.

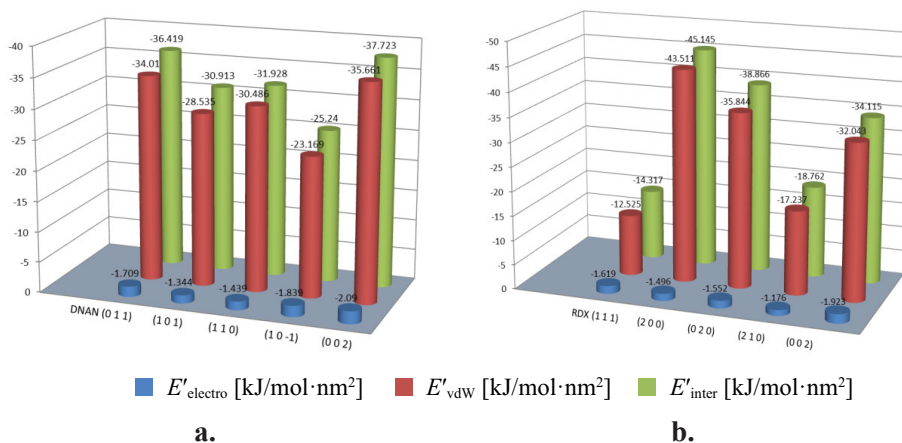


Figure 7. Comparison of the binding energies of the polymers on different crystal surfaces: (a) polymer on DNAN crystal surfaces; (b) polymer on RDX crystal surfaces

3.2 Fractured surface morphology

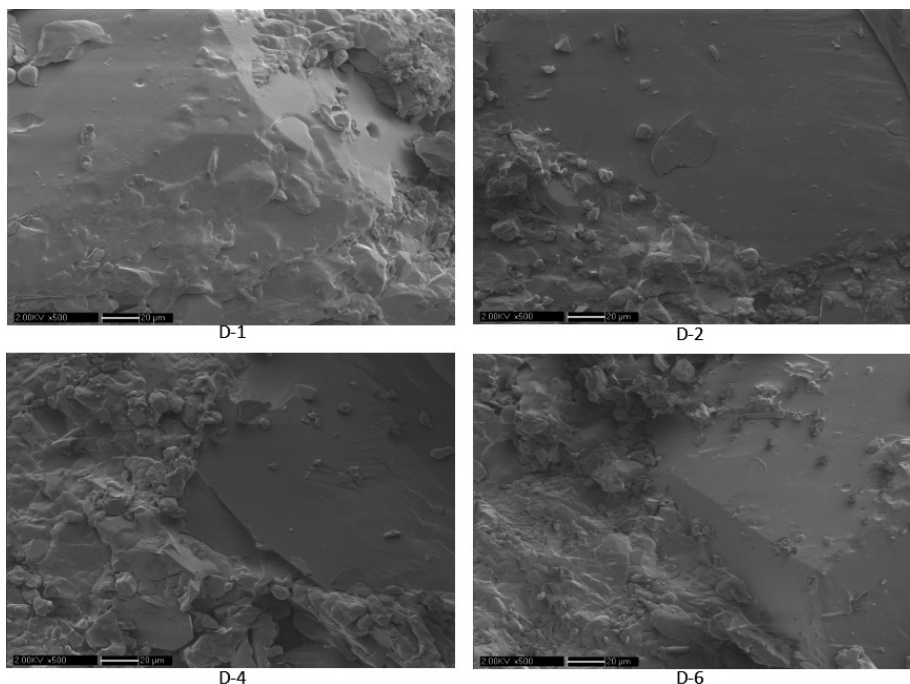


Figure 8. SEM images of DNAN/RDX energetic composites [200 kV, $\times 500$, 20 μm]

The micro-images of the interface can well demonstrate the strong interactions between the explosive and the polymeric modifiers. As shown in Figure 8, the molten DNAN solidified and formed the substrate, with different sizes of RDX particles inlaid on the DNAN substrate. The DNAN/RDX substrate surfaces were wrapped by the polymeric modifiers, forming strong interfacial interactions, which was consistent with the simulation results. The tight interfacial interactions can be the main positive factor for mechanical modification of energetic composites [36-38]. APER, which has good thermal compatibility with molten DNAN, can be evenly dispersed in the DNAN/RDX system, and the cross-linking reactions of the polymers [20-22] can form dense cross-linked network structures between the multi-phase systems, playing the role of binder in the energetic composites. Meanwhile, the coating effect of the polymers can synergize the DNAN/RDX system, forming energetic particles coated with polymers, filling the gaps between the particles and making the linking tight and close, modifying the overall mechanical performance.

3.3 Mechanical properties and cooperative mechanism

Table 4. Mechanical properties of DNAN energetic composites

Formulation	Polymer additives [wt.%]	Compressive strength [MPa]	Compressive elongation [%]	Tensile strength [MPa]	Tensile elongation [%]
RHD	0	20.63	0.290	2.16	0.034
D-1	1	27.71	0.433	2.57	0.027
D-2	2	35.16	0.467	3.12	0.047
D-4	4	41.26	0.477	3.33	0.048
D-6	6	43.92	0.634	4.59	0.049

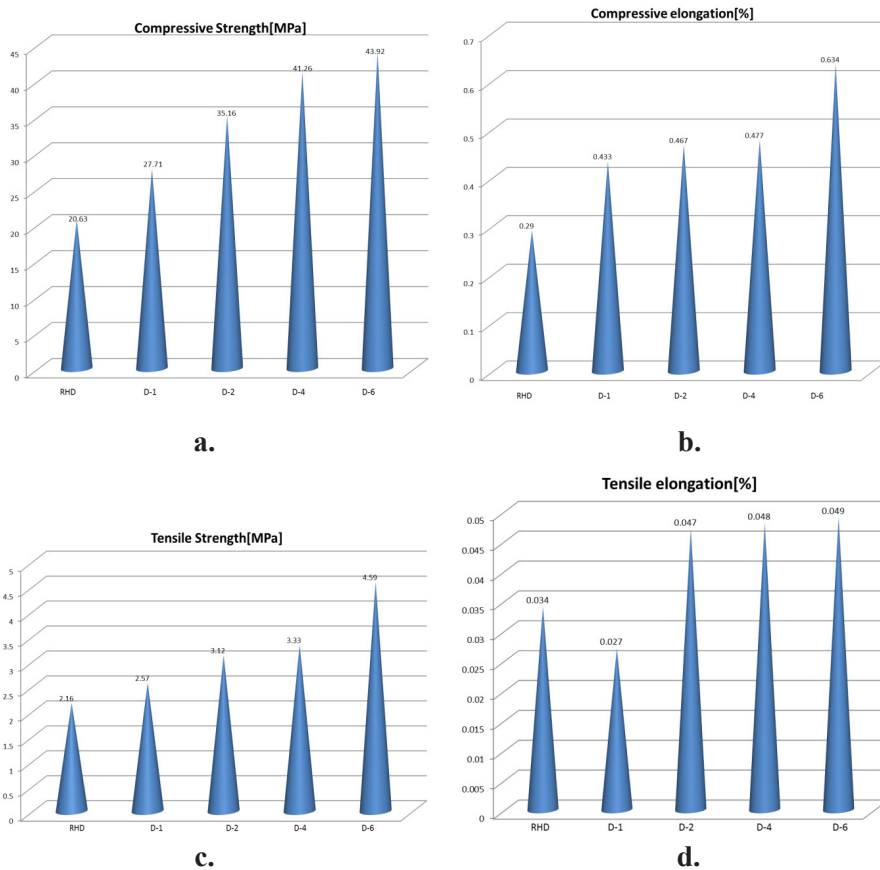


Figure 9. Comparison of the mechanical properties of DNAN energetic composites: (a) compressive strength, (b) compressive percentage elongation, (c) tensile strength, (d) tensile percentage elongation

From the mechanical test results shown in Table 4 and Figure 9, it may be seen that the addition of polymeric modifiers can significantly modify the mechanical properties of the DNAN/RDX system. Samples with 2%, 4% and 6% additives (which will not be used in industry) were compared with the 0% and 1% compositions to prove the effect that the polymer had on the mechanical properties, and showing that an elevated polymer content can increase the compressive/tensile strength and elongation. When adding APER, the compressive/tensile strengths were increased, for example the compressive strength of D-4 had increased to twice the value of RHD, demonstrating reinforcement of the strength for the energetic composites; and the compressive/tensile percentage elongation values of D-2, D-4 and D-6 are larger than that of RHD, showing improvement in the toughness of the energetic composites. As discussed above, strong interfacial interactions exist between the polymer and the DNAN surfaces, as the polymeric modifiers can tightly link with the explosive, thus these cooperative effects [20-22] can modify the mechanical performance of the whole energetic composite, preventing the DNAN energetic composite from being damaged by external loading, and satisfying the charging needs in weapon utility.

4 Conclusions

In this paper, the effects of interactions between the polymer and the explosive interfaces on the mechanical properties of the energetic composite were investigated both experimentally and theoretically, and conclusions can be drawn as follows:

- (1) Interfacial interaction energies were obtained from the MD simulations and energy calculations on the polymer/explosive-crystal solid interface models. It was found that strong interactions exist between the polymer and the DNAN/RDX interfaces, where van der Waals forces play the main part while electrostatic interactions have little effect. The energies along different crystal directions show anisotropy.
- (2) The experimental interface morphologies show tight linking between the polymers and the explosives, which demonstrates the strong interfacial interactions between the polymer and DNAN/RDX.
- (3) The mechanical tests show that the addition of APER can improve the mechanical strength and toughness, thus reinforcing the mechanical properties of the energetic composites for charges.

The conclusions are helpful in the formulation of DNAN-based energetic composites, which may be used in creating insensitive explosive castings.

Acknowledgements

Our group work was supported by the Innovation Foundation of the Institute of Chemical Materials, China Academy of Engineering Physics (Grant No. KJCX-201409). We acknowledge Dr. Yang Zhou, Dr. Jian Liu and Dr. Chaoyang Zhang for their attentive suggestions.

References

- [1] Fedoroff, B. T. *Dictionary of Explosives. Ammunition and Weapons*. Picatinny Arsenal, Technical Report 2510, **1958**.
- [2] Niles, J.; Doll, D. Development of a Practical Reduced Sensitivity Composition B Replacement. *32th Int. Annu. Conf. ICT*, Karlsruhe, Germany **2001**.
- [3] Patel, C. *Common Low-cost IM Explosive Program, Development of Next Generation Insensitive Munitions: A Success Story*. Picatinny Arsenal, NJ, DADC-TR-2010-225, **2011**.
- [4] Fung, V.; Schreiber, B. Large Scale Manufacturing of Insensitive Explosive IMX-104 at Holston Army Ammunition Plant. *2012 Insensitive Munitions and Energetic Material Technology Symposium*, Las Vegas, May 14-17, **2012**.
- [5] Headrick, S.; Price, D.; LeClaire, E. Development of an Efficient Alternative Process for DNAN Production. *2012 Insensitive Munitions and Energetic Material Technology Symposium*, Las Vegas, May 14-17, **2012**.
- [6] Fung, V.; Schreiber, B.; Patel, C.; Samuels, P.; Vinh, P.; Zhao, X. L. Process Improvement and Optimization of Insensitive Explosive IMX-101. *2012 Insensitive Munitions and Energetic Material Technology Symposium*, Las Vegas, May 14-17, **2012**.
- [7] Willson, A. Manufacturing of Explosive Ingredients and Compositions for the IM M795 Artillery Ammunition. *2007 Insensitive Munitions and Energetic Materials Symposium*, Miami, Florida, Oct. 15-18, **2007**.
- [8] Roos, B. The Characterization of IM Explosive Candidates for TNT Replacement. *2007 Insensitive Munitions and Energetic Materials Symposium*, Miami, Florida, Oct. 15-18, **2007**.
- [9] Singh, S. The Application of New IM Explosive Candidates in the M795 Projectile. *2007 Insensitive Munitions and Energetic Materials Symposium*, Miami, Florida, Oct. 15-18, **2007**.
- [10] Hunter, D. Comparison of Blast Performance of the IM Explosive PAX-28 Variations. *2007 Insensitive Munitions and Energetic Materials Symposium*, Miami, Florida, Oct. 15-18, **2007**.
- [11] Davies, P. J.; Provatias, A. *Characterization of 2,4-Dinitroanisole: an Ingredient for Use in Low Sensitivity Melt Cast Formulations*. Defence Science and Technology Organisation, Weapons System Division, Australia, DSTO-TR-1904, **2006**.
- [12] Moore, D. W.; Burkardt, L. A.; McEwan, W. S. Viscosity and Density of the Liquid

- System TNT-Picric Acid and Four Related Pure Materials. *J. Chem. Phys.* **1956**, *25*: 1235.
- [13] Qian, W., Chen, X. Z., Zhou, Y. The Interfacial Interaction and Diffusion Mechanism of Molten DNAN on High-Energetic Crystals: a Theoretical Investigation. *47th Int. Annu. Conf. ICT*, Karlsruhe, Germany **2016**.
- [14] Zhang, G. Q.; Dong, H. S. Review on Melt-Castable Explosives Based on 2,4-Dinitroanisole. (in Chinese) *Chin. J. Energ. Mater.* **2010**, *18*: 54-60.
- [15] Ma, Q.; Shu, Y. J.; Luo, G.; Chen, L.; Zheng, B. H.; Li, H. R. Toughening and Elasticizing Route of TNT Based Melt-Cast Explosives. (in Chinese) *Chin. J. Energ. Mater.* **2012**, *20*: 618-629.
- [16] Qian, W.; Zhang, C. Y.; Xiong, Y.; Zong, H. H.; Zhang, W. B.; Shu, Y. J. Thermal Expansion of Explosive Molecular Crystal: Anisotropy and Molecular Stacking. *Cent. Eur. J. Energ. Mater.* **2014**, *11*(1): 569-580.
- [17] Qian, W.; Shu, Y. J.; Li, H. R.; Ma, Q. The Effect of HNS on the Reinforcement of TNT Crystal: a Molecular Simulation Study. *J. Mol. Model.* **2014**, *20*: 2461.
- [18] Zhao, K.; Wang, H.; Wang, W.; Yang, F.; Liu, R.; Zhu, Y. Analysis of the Mechanical Properties of DNAN. (in Chinese) *Chin. J. Explo. Prop.* **2016**, *39*(4): 68-72.
- [19] Qian, W.; Shu, Y. J.; Li, H. R.; Ma, Q.; Wang, S. M.; Chen, X. Z. The Reinforcement of the TNT System by Newly-designed GAP-based Polyurethane-Urea: a Molecular Simulation Investigation. *Cent. Eur. J. Energ. Mater.* **2016**, *13*(2): 411-426.
- [20] Guest, H. R.; Adams, J. T.; Kiff, B. W. *Modified Acrolein-Pentaerythritol Resins*. Patent US 59681456A, **1959**.
- [21] Guest, H. R.; Adams, J. T.; Kiff, B. W. *Acrolein-Pentaerythritol Resins and Modifier Therefore*. Patent US 59682356A, **1959**.
- [22] Cai, J. L.; Gao, D. P.; Zheng, S. S.; Chi, Y. Curing Kinetics and Rheology Property of Acrolein-Pentaerythritol Resin System. (in Chinese) *Chin. J. Energ. Mater.* **2015**, *23*(6): 558-562.
- [23] Nyburg, S. C.; Faerman, C. H.; Prasad, L.; Palleros, D.; Nudelman, N. Structures of 2,4-Dinitroanisole and 2,6-Dinitroanisole. *Acta Crystallogr. Sect. C: Cryst. Struct. Commun.* **1987**, *43*: 686-689.
- [24] Choi, C. S.; Prince, E. The Crystal Structure of Cyclotrimethylenetrinitramine. *Acta Crystallogr.* **1972**, *28*(9): 2857-2862.
- [25] Accelrys Software Inc. *Materials Studio Release Notes, Release 6.1*, San Diego **2012**.
- [26] Sun, H. COMPASS: An ab Initio Forcefield Optimized for Condensed-Phase Applications – Overview with Details on Alkane and Benzene Compounds. *J. Phys. Chem. B* **1998**, *102*: 7338.
- [27] McQuaid, M. J.; Sun, H.; Rigby, D. Development and Validation of COMPASS Force Field Parameters for Molecules with Aliphatic Azide Chains. *J. Comp. Chem.* **2004**, *25*(1): 61-71.
- [28] Bravais, A. *Etudes Crystallographiques* (the 2011 ed., Nabu Press), Academie des Sciences, Paris, **1913**; ISBN 1246427524.
- [29] Friedel, G. Studies on the Law of Bravais. (in French) *Bull. Soc. Fr. Mineral.* **1907**, *30*: 326-455.

- [30] Donnay, J. D. H.; Harker, D. A New Law of Crystal Morphology Extending the Law of Bravais. *Am. Mineral* **1937**, *22*: 446-467.
- [31] Verlet, L. Computer Experiments on Classical Fluids. I. Thermodynamical Properties of Lennard-Jones Molecules. *Phys. Rev.* **1967**, *159*: 98-103.
- [32] Ewald, P. P. The Calculation of Optical and Electrostatic Lattice Potentials. (in German) *Ann. Phys. (Leipzig)* **1921**, *64*: 253.
- [33] Karasawa, N.; Goddard, W. A. Acceleration of Convergence for Lattice Sums. *J. Phys. Chem.* **1989**, *93*: 7320-7327.
- [34] Andersen, H. C. Molecular Dynamics Simulations at Constant Pressure and/or Temperature. *J. Phys. Chem.* **1980**, *72*: 2384.
- [35] Berendsen, H. J. C.; Postma, J. P. M.; van Gunsteren, W. F.; DiNola, A.; Haak, J. R. Molecular Dynamics with Coupling to an External Bath. *J. Chem. Phys.* **1984**, *81*: 3684-3690.
- [36] Qiu, L.; Xiao, H. M. Molecular Dynamics Study of Binding Energies, Mechanical Properties, and Detonation Performances of Bicyclo-HMX-based PBXs. *J. Hazard. Mater.* **2009**, *164*: 329-336.
- [37] Ma, X. F.; Xiao, J. J.; Huang, H.; Ju, X. H.; Li, J. S.; Xiao, H. M. Simulative Calculation of Mechanical Property, Binding Energy and Detonation Property of TATB/Fluorine-Polymer PBX. *Chin. J. Chem.* **2006**, *24*: 473-477.
- [38] Zhu, W.; Xiao, J. J.; Zhu, W. H.; Xiao, H. M. Molecular Dynamics Simulations of RDX and RDX-based Plastic Bonded Explosives. *J. Hazard. Mater.* **2009**, *164*: 1082-1088.
- [39] *Explosive Test Method*. National Military Standard of China, GJB/772A-97, **1997**.
- [40] Ma, Q.; Wang, P. S.; Luo, G.; Wen, M. P.; Gao, D. Y.; Zheng, B. H.; Shu, Y. J. Microstructure, Mechanical and Detonation Properties of Elastomeric Micro/Ultrafine-Rubber Modified TNT-based Molten Energetic Composites. *Cent. Eur. J. Energ. Mater.* **2015**, *12*(4): 723-743.